

# Thermal Characterization of SBR/NBR Blends Reinforced with a Mesoporous Silica

Leon D. Perez,<sup>1,2</sup> Betty L. Lopez<sup>2</sup>

<sup>1</sup>Departamento de química, Pontificia Universidad Javeriana, Bogotá, Bogota, D.C. Colombia

<sup>2</sup>Grupo Ciencia de los Materiales, Universidad de Antioquia, Medellín, Antioquia, Colombia

Received 9 September 2010; accepted 20 September 2011

DOI 10.1002/app.35689

Published online 17 January 2012 in Wiley Online Library (wileyonlinelibrary.com).

**ABSTRACT:** In this article, blends of styrene butadiene rubber (SBR) and acrylonitrile butadiene rubber (NBR) filled with a mesoporous silica are characterized by using scanning electron microscopy (SEM), dynamic mechanical analysis, and differential scanning calorimetry. According to the variation of the glass transition temperature with the composition of the blends, it is deduced that the compatibility of SBR and NBR is reduced in the presence of

mesoporous silica. Analysis of the morphology of the composites by SEM shows that the dispersion of the filler is improved in the presence of NBR which is an indicative that this elastomer interacts stronger with silica than SBR. © 2012 Wiley Periodicals, Inc. *J Appl Polym Sci* 125: E327–E333, 2012

**Key words:** mesoporous silica; rubber blend; compatibility

## INTRODUCTION

Blending of elastomers with different properties has been extensively used to obtain materials with improved performance. For instance, blends of styrene butadiene rubber (SBR) and acrylonitrile butadiene rubber (NBR) are promissory for the design of devices with better chemical properties.<sup>1–3</sup> NBR is a polar elastomer, which makes it highly resistant to nonpolar substances such as hydrocarbons and oils. NBR also presents good mechanical and tribological properties. On the other hand, SBR is a low-polar elastomer; therefore, it is resistant to polar substances such as water and alcohols. SBR also has larger elasticity and is less expensive than NBR.

Nevertheless, the preparation of blends based on NBR and SBR is challenging due to their poor compatibility. As an alternative, the use of additives such as unsaturated polyester resin,<sup>4</sup> polyglycidylmethacrylate-g-butadiene rubber,<sup>5</sup> polyacrylonitrile,<sup>6</sup> NBR grafted with cellulose acetate, and methylmethacrylate<sup>7</sup> has been reported to improve their compatibility. Some fillers can also compatibilize these kind of blends; for instance, Essawy reported that montmorillonite increases the degree of compatibil-

ity between NBR and SBR. This conclusion was supported by changes in the curing behavior and thermal properties of the blends after the reinforcement.<sup>2</sup>

According to Lipatov et al., the filler ability to act as a compatibilizer rises from the adsorption of polymer chains on its surface, and the subsequent reduction of their mobility prevents the phase separation.<sup>8</sup> A thermodynamic description of the effect that a filler has on the miscibility of polymer blends can be found elsewhere.<sup>9</sup>

The degree of miscibility in polymer blends depends on the characteristics of the components. In the case of amorphous polymers, the glass transition can be used to monitor miscibility. For instance, completely immiscible blends exhibit the glass transitions corresponding to the individual components, whereas miscible blends exhibit a single glass transition.<sup>10</sup>

The scenario is more complex in the case of partially miscible blends; a greater or lesser degree of compatibility depends on the size of the domains. Conventional techniques such as polarized light microscopy, atomic force microscopy,<sup>11</sup> scanning electron microscopy (SEM),<sup>12</sup> and transmission electron microscopy<sup>13</sup> have been extensively used with this purpose. Other alternative is to determine the size and composition of the interphase by techniques such as modulated temperature differential scanning calorimetry (MTDSC), and magnetic nuclear resonance. Interphase is taken as the region that links the domains and presents properties completely different to each individual component.<sup>14,15</sup>

Correspondence to: L. D. Perez (leon.perez@javeriana.edu.co).

Contract grant sponsors: Universidad de Antioquia, Colciencias, Colombia (Apoyo a la comunidad científica nacional a través de becas para estudios doctorales) (LDP)

TABLE I  
Composition of the Samples

Components (phr)	S0	S25	S50	S75	S100
SBR	0	25	50	75	100
NBR	100	75	50	25	0
Silica	60	60	60	60	60
Zinc oxide	5	5	5	5	5
Stearic acid	1	1	1	1	1
Agerite resin D	2	2	2	2	2
CBS	2	2	2	2	2
ZDEC	0.8	0.8	0.8	0.8	0.8

CBS, *N*-cyclohexyl-2-benzothiazole-sulfenamide; ZDEC: zinc diethyl carbamate; Agerite Resin D, 2,2,4-trimethyl-1,2-hydroquinolina.

The purpose of this work is to characterize the morphology and thermal behavior of blends based on NBR/SBR filled with mesoporous silica nanoparticles and determine their effect on the blend compatibility. According to previous studies, mesoporous silica fillers interact stronger with rubbery matrices compared to other nonporous fillers, because those materials have larger surface area and an organized porous structure.<sup>16–19</sup>

## EXPERIMENTAL

### Materials

SBR 1502 with 23.55 wt % styrene ( $M_w = 3.3 \times 10^5$  Da, polydispersity (PD) = 3.4, Polysar), NBR with 33 wt % Acrylonitrile ( $M_w = 2.45 \times 10^5$  Da, PD = 3.5, Krynac 3345, Bayer), and vulcanization additives, 2,2,4-trimethyl-1,2-hydroquinoline (Agerite resin D), zinc diethyl dithiocarbamate, and *N*-cyclohexylbenzothiazole-2-sulphenamide were supplied by Monsanto. Bis(3-triethoxysilylpropyl) tetrasulfide (TESPT) purchased from Degussa was used as received. Hydrofluoric acid (HF) was supplied by Sigma.

Mobile crystalline material (MCM)-41 mesoporous silica sample was synthesized following the procedure previously reported.<sup>16</sup> The material showed mesoporous characteristics; its specific surface area and pore diameter determined by nitrogen adsorption were 843.5 m<sup>2</sup>/g and 2.7 nm, respectively.

### Mesoporous silica modification

The modification of silica with TESPT was carried out by impregnation from a solution of the silane coupling agent as follows; a sample of 10 g of silica, previously dried at 250°C during 24 h, was dispersed in 200 mL of acetone; then 0.8 g of TESPT were added. The resulting dispersion was kept under stirring for 24 h at room temperature in a closed container; after this time, the acetone was slowly evaporated at 30°C. Then remaining material

was heated at 100°C for 24 h under inert atmosphere.

### Composite preparation

Filled elastomer blends were prepared in a two rolls open mill, in three stages: (1) homogenization of NBR/SBR blends, (2) incorporation of the filler into the homogenized blends, and (3) addition of the vulcanization reagents. Details of the composition are listed in Table I. The curing times were determined by DSC in a TA Instruments Q100 calorimeter under isothermal conditions at 150°C, the curing time was determined as the time at which the reaction degree was 90%. The vulcanization of the samples was carried out at 150°C and 21 MPa, in a compression-molding machine, to obtain films with thickness around 1 mm.

The samples are named as: "S # \_ #," the first and the second number refer to the content of SBR and silica in the blend, respectively. A "T" at the end indicates that the silica was modified with TESPT. Nonvulcanized samples (without any vulcanization additive) were treated at the conditions used for the vulcanization, i.e., annealing at 150°C under pressure (21 MPa) for 15 min.

### Sample characterization

The morphology of the composites was examined by SEM in a FEI Phillips model XL30. The elastomeric samples were frozen in liquid nitrogen, fractured, and covered with gold.

MTDSC analyses were carried out as follows: the thermal history of the samples was erased by heating from room temperature up to 150°C at 20°C/min and then cooled to -90°C at 20°C/min. The thermograms were acquired heating at an overall rate  $\beta = 3^\circ\text{C}/\text{min}$ , modulated at  $\pm 1^\circ\text{C}$  every 60 s. The experiments were carried out in Q100 TA Instruments.

Dynamic mechanical thermograms were collected from -100 to 50°C, heating at 3°C/min at 1 Hz. The measurements were performed using the extension film clamp in a dynamic mechanical analysis (DMA; Diamond, PerkinElmer).

## RESULTS AND DISCUSSION

### Analysis of filler dispersion by SEM

According to Figure 1(A), silica in composite S100\_60 is poorly dispersed; aggregates around 1  $\mu\text{m}$  are predominant, and individual particles are rarely noticed. For the composite S0\_60, Figure 1(B), the size of the aggregates is comparatively reduced, and some individual particles are observed. The

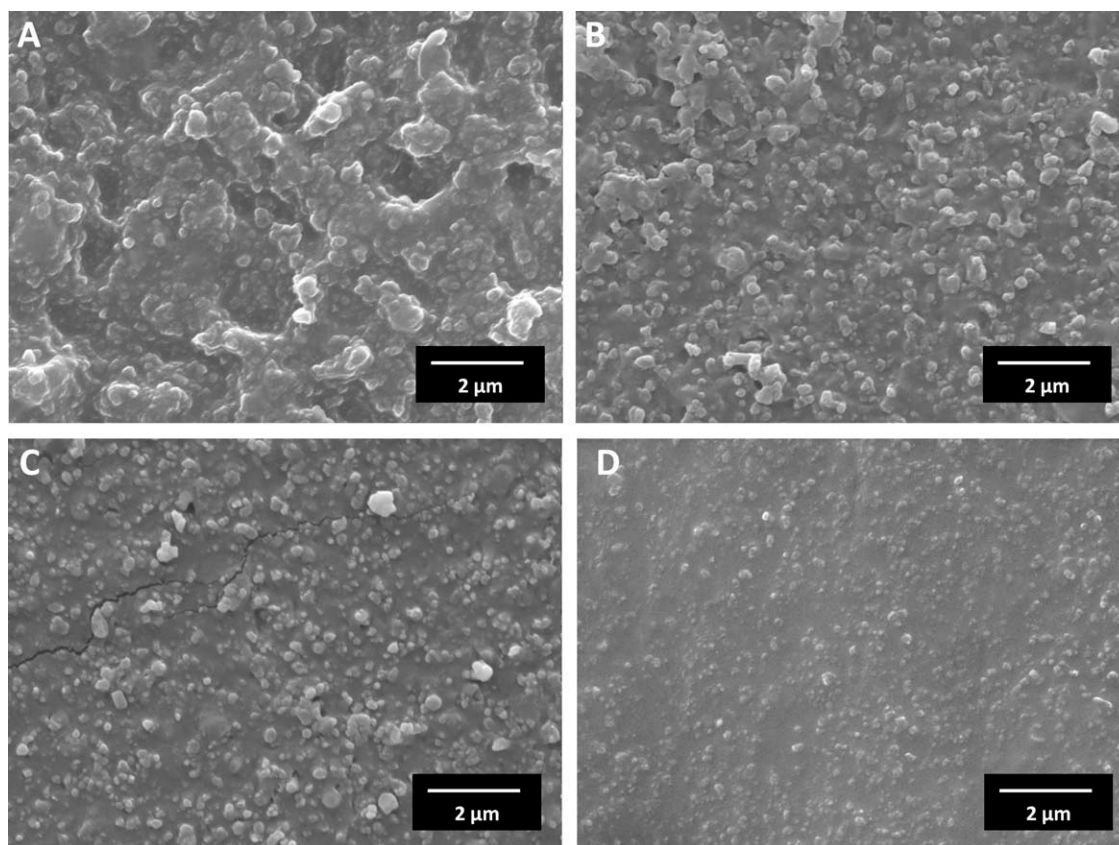


**Figure 1** SEM images for the nonvulcanized composites: (A) S100\_60, (B) S0\_60, (C) S50\_60, and (D) S50\_60T.

dispersion of silica in the blends of polymers is similar to that observed for S0\_60; as an illustration Figure 1(C) shows the SEM image for the sample S50\_60. On the other hand, the dispersion was significantly improved by the modification of silica particles with TESPT [Fig. 1(D)]; in that composite, silica filler seems to be in the form of individual particles and aggregates smaller than 500 nm.

In elastomer-based composites, the dispersion of the filler and hence the morphology are mainly governed by attractive forces between the filler particles such as hydrogen bonds and interactions between the filler particles and the polymer matrix. They both are competitive, a good dispersion of the filler is achieved when silica-silica interactions are weaker than filler-polymer interactions. For instance, when silica is modified with TESPT, the improvement of silica dispersion is due to the decrease of silanol groups density and a concomitant reduction of the interactions between the particles. Also the presence of those voluminous groups at silica surface exerts a steric hindrance to the silica particles aggregation. Similarly, raw silica disperses better in NBR and blends containing it than in SBR; the silanol groups on its surface interact stronger with nitrile groups on NBR than with the corresponding phenyl groups on SBR.

### Thermal characterization of the nonvulcanized composites

To study the effect that the filler and blend composition have on the thermal behavior of the composites, DMA and DSC were used to characterize the nonvulcanized samples. The  $T_g$  values determined by both techniques are listed in Tables II and III, the results show that the  $T_g$  varies with the method of measurement owing to the broad temperature region of the transition and also to the dependence of that transition on experimental conditions such as heating rate and modulation and deformation

**TABLE II**  
Glass Transition Temperatures for Nonvulcanized Samples, Measured by DMA as the Temperature at the Maximum of  $E''$

Blend	No filler added		Silica (60 phr)	
	$T_g$ (°C)		$T_g$ (°C)	
	SBR	NBR	SBR	NBR
S0		-24.0		-26.8
S25	-54.4	-22.17	-60.8	-27.3
S50	-55.6	-27.4	-58.6	-26.8
S50_60T			-55.7	-33.0
S75	-58.7	-25.8	-52.7	
S100	-59.4		-53.4	

**TABLE III**  
Glass Transition Values for Nonvulcanized Samples Measured by MTDSC

Blend	No filler added		Silica (60 phr)	
	$T_g$ (°C)		$T_g$ (°C)	
	SBR	NBR	SBR	NBR
S0		-34.2		-32.9
S25	-54.8	-33.3	-55.1	-32.8
S50	-55.1	-33.2	-54.3	-33.5
S50_60T			-54.1	-34.1
S75	-55.1	-32.5	-53.9	
S100	-55.5		-54.1	

frequencies in MTDSC and DMA, respectively. The following discussions will be based on the  $T_g$  values taken as the temperature of the maximum of  $E''$  versus temperature curves given that those values are more obvious than the corresponding data obtained from DSC thermograms.

Figure 2(A) shows the variation of  $T_g$  measured by DMA as a function of the content of SBR for the unfilled blends. It is observed that the  $T_g$  values of the elastomers tend to get closer; this behavior indicates that the polymers are slightly compatible. Probably, the interaction between SBR and NBR is facilitated by the presence of butadiene rich segments in the copolymers.

On the reinforcement [Fig. 2(B)], the  $T_g$  of SBR increases, whereas that of NBR decreases compared with the corresponding unfilled polymers. In the filled blends, the  $T_g$  of the SBR phase depends on the concentration of NBR; at low contents, the  $T_g$  of SBR is close to the value obtained for S100\_60. When the concentration of NBR increases, the  $T_g$  of SBR decreases and becomes close to the value obtained for the unfilled elastomer. The  $T_g$  associated to NBR remains almost constant, and near the

$T_g$  of the composite S0\_60; excepting the composite S75\_60, which does not exhibit any transition associated to the NBR; this behavior was also corroborated by MTDSC, data in Table III.

NBR with low acrylonitrile content synthesized by emulsion polymerization, as the type used in this study, is structurally heterogeneous, and composed by chain segments with different acrylonitrile contents.<sup>20</sup> In the presence of silica, the acrylonitrile rich segments are preferentially adsorbed on its surface, which reduces their mobility and prevents the occurrence of cooperative motions. Consequently, butadiene rich segments, which are more flexible, remain in the bulk, and thus the filled NBR presents a lower  $T_g$ .

In the case of SBR, as the amount of NBR increases the probability of the SBR chains to interact with the filler decreases. For example, SBR in the composite S100\_60 presents a higher  $T_g$  than S25\_60. It is because the nitrile groups on the NBR interact stronger with silica than the phenyl groups on the SBR.<sup>21</sup>

Tables II and III also show the  $T_g$  of the composite S50\_60T, which contains silica chemically modified with TESPT. Contrary to above described behavior, with the addition of TESPT-graft-silica particles (data in Tables II and III) the  $T_g$  of SBR and NBR in the blend get closer, which is related to a slight miscibility of the elastomers also observed in the case of nonfilled blends.

TESPT is widely used to impart dispersion of silica in rubber composites and improve their performance, especially in tire applications. This kind of silane is able to react with both, silica surface and rubber chains during the vulcanization. Before the vulcanization, the silane attached to the surface of silica particles lessens their polarity; and, therefore, the favorability of NBR for being adsorbed to the filler surface is also lowered.

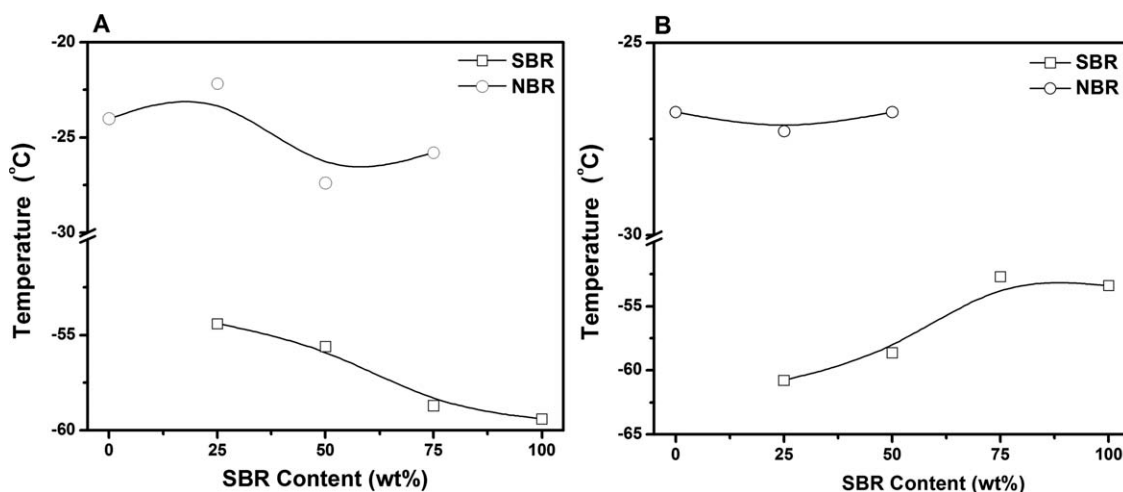


**Figure 2** Variation of the glass transition temperatures measured by DMA as the maxima of  $E''$ , for the different composition of the blends: (A) without filler and (B) with 60 phr of silica filler.

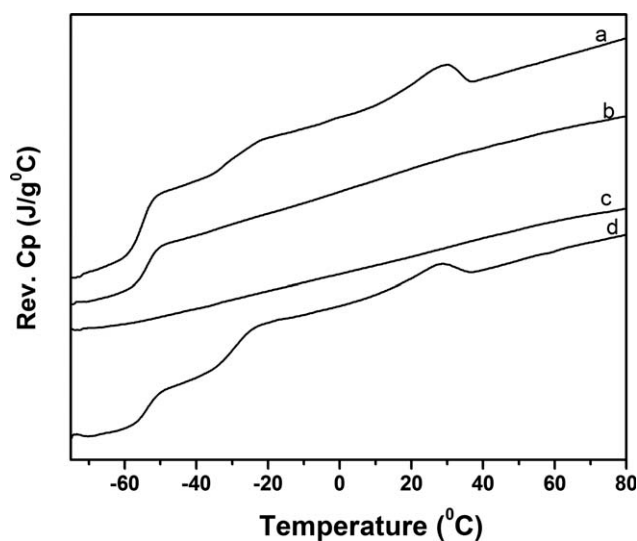


**Figure 3** MTDSC thermograms for (a) S75\_0, (b) S75\_60, and (c) S75\_60 bound rubber and (d) S75\_60 bound rubber etched with HF.

Figure 3 shows the MTDSC thermograms for the blend that contains 75 wt % of SBR without any filler and with 60 phr of silica and the corresponding fraction of bound rubber; which is obtained thoroughly extracting the bulk rubber from the composite S75\_60 with toluene, and a sample of the bound rubber washed with HF to remove the silica. The unfilled blend presents the distinctive transitions of both elastomers, the filled blend only shows the transition due to the SBR phase, and the thermogram of the bound rubber does not show any transition. However, the thermogram corresponding to the bound rubber etched with HF shows the transitions also seen in the unfilled blend, indicating that the polymer segments recovered the mobility after silica extraction. These results provide additional evidence to confirm that in SBR/NBR blends reinforced with silica, the polymer chains interacting

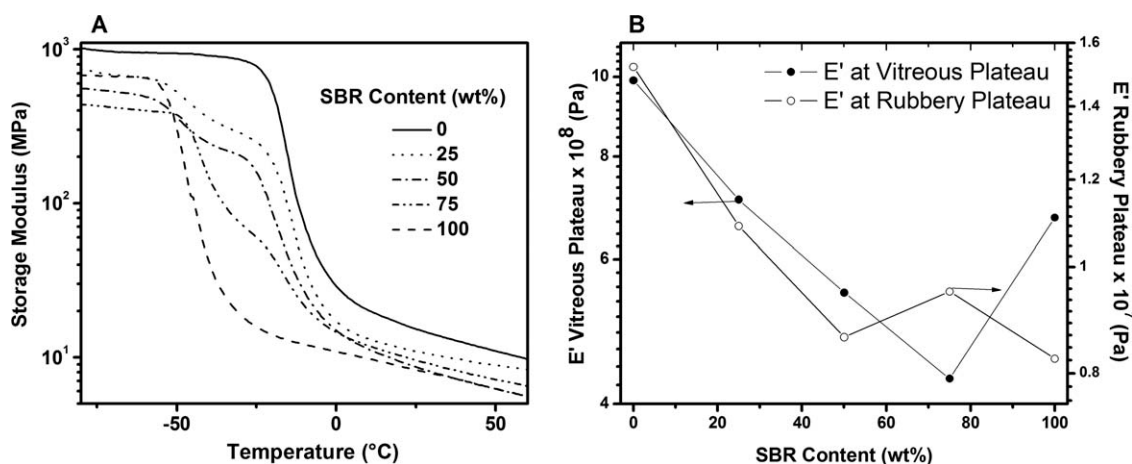
strongly with the filler do not present glass transition.

### Dynamic mechanical analysis of the vulcanized blends

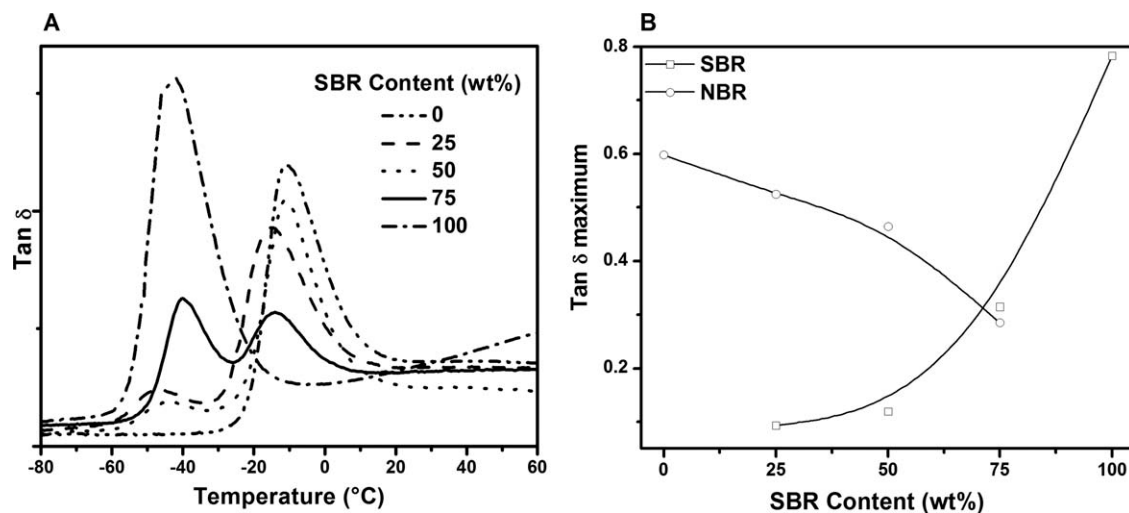
Dynamic mechanical properties such as storage modulus ( $E'$ ) and damping constant ( $\tan \delta$ ) of the vulcanized composites were evaluated. Figure 4(A) shows the variation of  $E'$  with temperature for the silica-filled blends. The blends exhibit three plateaus and two transition regions; the first plateau corresponds to the glassy state of both polymers; in the second, SBR is rubbery and NBR is still a glass, and in the third one, both are rubbery. The transition regions, denoted by a progressive decreasing of  $E'$  with the temperature, are due to the occurrence of the glass transition associated to each elastomer.

Figure 4(B) shows the variation of storage modulus in both, the glassy and rubbery state, at  $-75$  and  $25^\circ\text{C}$ , respectively, as a function of the SBR content. In the glassy plateau, the maximum value of  $E'$  is observed for the vulcanized composite containing only NBR, decreases with the incorporation of SBR into blends and augments for the SBR alone. The NBR chains are stiffer than SBR, and consequently, as the NBR content decreases, the composite rigidity is lowered. Additionally, the presence of NBR improves the dispersion of silica particles which agrees with previous reports.<sup>22</sup> The increase in modulus for the composite S100\_60 is attributable to the agglomeration of filler particles that increases the stiffness, particularly at low-amplitude deformations.<sup>23,24</sup>

In the rubbery region, a similar behavior was observed, and the value of the modulus is maxima in the case of NBR and decreases for the blends. Except for composite that contains 75 wt % of SBR whose  $E'$  is higher than the corresponding value for the composite that contains 50 wt % of SBR.



**Figure 4** Dynamic mechanical analysis results for the vulcanized samples. (A) plots as function of the temperature for all the compositions and (B) storage modulus in the vitreous and rubbery region as a function of the blends composition.



**Figure 5** Dynamic mechanical analysis results for the vulcanized samples. (A)  $\tan \delta$  plots as function of the temperature for all the compositions and (B) maximum of  $\tan \delta$  for each glass transition as function of the blend composition.

According to the previous results, at that composition, most of the NBR in the blend is adsorbed at the silica surface; it increases the effective volume of the filler and therefore the elastic modulus of the composite.

Plots of  $\tan \delta$  versus temperature for the reinforced blends are shown in Figure 5(A). Generally, for immiscible binary blends,  $\tan \delta$  exhibits two maxima,<sup>25</sup> whereas completely miscible blends show a single peak associated to the glassy relaxation of the resulting supramolecular structure.<sup>26</sup> According to Figure 5(A), for the blends, the position of the peaks due to the glassy relaxation of each component is shifted to lower temperature in comparison to the respective filled polymers. In the case of the composite S75\_60, the value of  $\tan \delta$  in the temperature range between the peaks, due to the glass transition of each phase in the blend, is larger than for

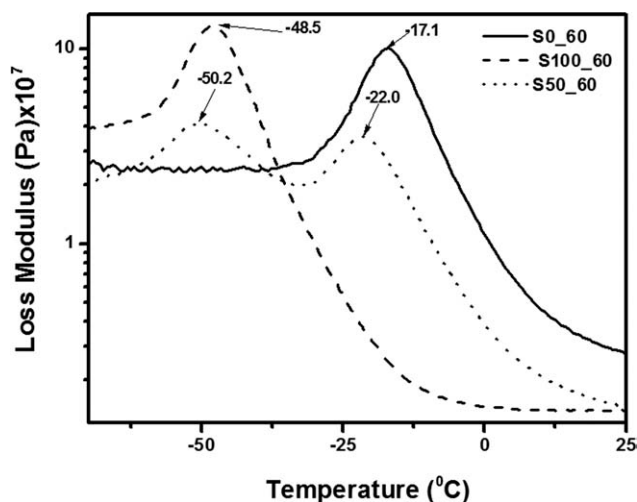


**Figure 6** Loss modulus plots for the samples S50\_60 and the corresponding filled polymers.

the individual rubbers. This behavior could indicate that at this composition a diffuse interphase SBR/NBR is established; probably, it is because in this composite, the nitrile-rich segments of the NBR are adsorbed at the silica surface and remaining less polar segments are more compatible with SBR.

The height of  $\tan \delta$  peaks for SBR in the filled blends, shown in Figure 5(B), decreases drastically with increasing the concentration of NBR. Probably, when the SBR goes from vitreous to rubbery state (at the glass transition), the NBR is still glassy so that rigid domains decrease the segmental mobility of the SBR chains, and their free volume. The NBR has a smaller reduction than that observed for the SBR, which implies that the presence of SBR does not have a marked effect on the mobility of NBR chains.

Although the discussion on the glass transition behavior in the previous sections was focused on nonvulcanized composites to avoid effects due to crosslinking, the results obtained for the vulcanized samples showed the same tendency. For example, Figure 6 compares the loss modulus plots for the vulcanized composites containing 50 wt % of each elastomer and the individual vulcanized filled elastomer. On the presence of silica, the glass transition temperature of both phases in the blend decreases, which is due to the adsorption of acrylonitrile-rich segments of NBR at the silica surface, as discussed above.

## CONCLUSIONS

The glass transition temperature of the elastomers showed to depend on both, the presence of filler and the blend composition. In the unfilled blends, the variation of the  $T_g$  of the elastomers with the composition indicates that NBR and SBR are slightly compatibles. On the other hand, the incorporation of

mesoporous silica decreases the compatibility of the elastomers. This behavior is attributed to the highest affinity of NBR for the silica surface, which also explains the improvement of the dispersion of filler particles in the presence of this elastomer.

Bound rubber in the composites is stiff and does show any transition, which is due to the conformational restrictions imposed by the silica particles. A large amount of bound rubber increases the effective volume of the filler, and thus the stiffness of the composite also increases.

## References

1. Rahiman, K. H.; Unnikrishnan, G. *J Polym Res* 2006, 13, 297.
2. Essawy, H.; El-Nashar, D. *Polym Test* 2004, 23, 803.
3. Kucukpinar, E.; Doruker, P. *Polymer* 2006, 47, 7835.
4. Mansour, S. H.; Tawfik, S. Y.; Youssef, M. H. *J Appl Polym Sci* 2002, 83, 2314.
5. Botros, S. H.; Moustafa, A. F.; Ibrahim, S. A. *J Appl Polym Sci* 2006, 99, 1559.
6. Darwish, N. A.; Shehata, A. B.; El-Megeed, A. A. A.; Halim, S. F.; Mounir, A. *Polym-Plast Technol Eng* 2005, 44, 1297.
7. Khalf, A. I.; Nashar, D. E. E.; Maziad, N. A. *Mater Design* 2010, 31, 2592.
8. Lipatov, Y. S.; Nesterov, A. E.; Ignatova, T. D.; Nesterov, D. A. *Polymer* 2001, 43, 875.
9. Lipatov, Y. S. *Prog Polym Sci* 2002, 27, 1721.
10. Brostow, W.; Chiu, R.; Kalogeras, I. M.; Vassilikou-Dova, A. *Mater Lett* 2008, 62, 3152.
11. Tsou, A. H.; Waddell, W. H. *KGK-Kautschuk Gummi Kunststoffe* 2002, 55, 382.
12. Dias, D. S.; Crespi, M. S.; Kobelnik, M.; Ribeiro, C. A. *J Therm Anal Calorim* 2009, 97, 581.
13. Radovanovic, E.; Carone, E.; Goncalves, M. C. *Polym Test* 2004, 23, 231.
14. Park, S. J.; Seo, M. K. *Polymer (Korea)* 2005, 29, 221.
15. T. L. Rocha, Rosca, C.; Schuster, R. H.; Jacobi, M. M. *J Appl Polym Sci* 2007, 104, 2377.
16. Perez, L. D.; Sierra, L.; López, B. L. *Polym Eng Sci* 2008, 48, 1986.
17. Perez, L. D.; Lopez, J. F.; Orozco, V. H.; Kyu, T.; Lopez, B. L. *J Appl Polym Sci* 2009, 111, 2229.
18. Perez, L. D.; Giraldo, L. F.; Brostow, W.; Lopez, B. L. *E-Polymers* 2007, 1, 29.
19. Perez, L. D.; Giraldo, L. F.; Lopez, B. L.; Hess, M. *Macromol Symp* 2006, 245–246, 628.
20. Ambler, M. R. *J Polym Sci Part A: Polym Chem* 1973, 11, 1505.
21. L. D. Pérez, Florez, E.; Mark, J. E.; López, B. L. *Polym Int* 2009, 58, 811.
22. Choi, S. S. *J Appl Polym Sci* 2001, 79, 1127.
23. Kohls, D. J.; Beaucage, G. *Curr Opin Solid State Mater Sci* 2002, 6, 183.
24. Gauthier, C.; Reynaud, E.; Vassoille, R.; Ladouce-Stelandre, L. *Polymer* 2004, 45, 2761.
25. Papke, N.; Karger-Kocsis, J. *Polymer* 2001, 42, 1109.
26. Varughese, K. T.; Nando, G. B.; De, P. P.; De, S. K. *J Mater Sci* 1988, 23, 3894.